Single-Site Localization Based on a New Type of Fingerprint for Massive MIMO-OFDM Systems

Xiaoyu Sun, *Student Member, IEEE*, Xiqi Gao, *Fellow, IEEE*, Geoffrey Ye Li, *Fellow, IEEE*, and Wei Han

***Abstract*—Localization for mobile devices is drawing increasing interest from both industry and academia as location-based services spring up in recent years. For rich scattering environments, such as urban areas and indoor corridors, fingerprint-based localization techniques are very promising. In this paper, we propose a fingerprint-based single-site localization method for massive multiple-input multiple-output (MIMO) orthogonal frequency-division multiplexing (OFDM) systems. A new angle delay channel power matrix fingerprint is extracted from instantaneous channel state information by taking full advantage of the high resolution in the angle and delay domains for massive MIMO-OFDM systems. A new fingerprint similarity criterion is proposed to facilitate localization. Based on the new criterion, an efficient location estimation method is developed. To reduce storage overhead and matching complexity, we also propose a fingerprint compression method and a two-stage fingerprint clustering algorithm for database preprocessing. Numerical results demonstrate the desirable performance of the proposed localization method.**

***Index Terms*—Fingerprint localization, massive MIMO-OFDM, fingerprint compression, database preprocessing.**

I. Introduction

DRIVEN by both security and commercial demands, wireless localization for mobile devices is drawing increasing interest from both industry and academia as location-based services (LBSs) spring up in recent years [1]. In order to bring out accurate location information timely, many techniques have been developed based on the global positioning system (GPS) as well as wireless networks [1], [2], most of which depend on the assumption that the wireless signals propagate along the line-of-sight (LOS). The locations are then calculated via simple triangulation based on multiple base station (BS) cooperation with measurements of receiving signal strength (RSS), angle-of-arrival (AOA), time-of-arrival (TOA), etc.

Massive multiple-input multiple-output (MIMO) orthogonal frequency-division multiplexing (OFDM) systems are promising for the upcoming 5G wireless communications for their enormous potential in spectral efficiency and power efficiency with simple signal processing [3]–[5]. With a larger scale antenna array and wide bandwidth adopted in massive MIMO-OFDM systems, BSs can easily acquire higher multipath resolution in the angle and delay domains. In recent years there has been a growing interest in massive MIMO localization, which is taken as a key enabler for high accuracy localization. In [6] and [7], a multiple AOAs estimation approach via rotational invariance technique (ESPRIT) has been proposed for two-dimensional localization. In [8], a time-frequency based multiple signal classification (MUSIC) method has been applied to massive MIMO systems for direction of arrival (DOA) estimation.

However, most localization requirements emerge at urban areas and indoor corridors, where the wireless signals usually propagate along multipath from different scatters and LOS condition is not available. As a result, the accuracy of wireless localization degrades in these rich scattering scenarios. Worse still, the triangulation calculation requires multiple base stations (BSs) cooperation, which may cause extra information exchange overhead and latency. To overcome the limitations in conventional localization techniques, a possible strategy is to enhance the triangulation method by distinguishing or recovering the AOA of LOS path from BS side. In [9], a joint TOA and AOA localization has been presented by converting none-line-of-sight (NLOS) AOA into LOS AOA through virtual stations. TOA can also be used to restrict the AOAs to a feasible area for direct localization [10]. Another option to make the utmost of the high multipath resolution is to escape from the shackles of conventional triangulation method by exploiting fingerprint technique [11]–[23].

The key idea of fingerprint technique exploits the fact that the wireless channel from the mobile device to the BS is uniquely determined by the scattering environment around the location of the mobile device. Some critical parameters from the wireless channel, referred to as a fingerprint corresponding to the location, are first extracted to uniquely describe the multipath information for each location. Then the localization problem is transformed into a pattern recognition problem, including fingerprint extraction, fingerprint matching, and location estimation.

Manuscript received September 14, 2017; revised January 17, 2018; accepted February 18, 2018. Date of publication March 7, 2018; date of current version July 16, 2018. This work was supported by National Natural Science Foundation of China under Grants 61320106003, 61471113, 61521061, 61631018, and 61761136016, National Science and Technology Major Project of China under Grant 2017ZX03001002-004, and the Huawei Cooperation Project. The work of X. Sun was supported in part by the China Scholarship Council. The review of this paper was coordinated by X. Wang. *(Corresponding author: Xiqi Gao.)*

X. Sun and X. Q. Gao are with the National Mobile Communications Research Laboratory, Southeast University, Nanjing 210096, China (e-mail: sunxiaoyu@seu.edu.cn; xqgao@seu.edu.cn).

G. Y. Li is with the School of Electrical and Computer Engineering, Georgia Institute of Technology, Atlanta GA 30332-0250 USA (e-mail: liye@ece.gatech.edu).

W. Han is with the Huawei Technologies, Co. Ltd., Shenzhen 518057, China (e-mail: wayne.hanwei@huawei.com).

Color versions of one or more of the figures in this paper are available online at http://ieeexplore.ieee.org.

Digital Object Identifier 10.1109/TVT.2018.2813058

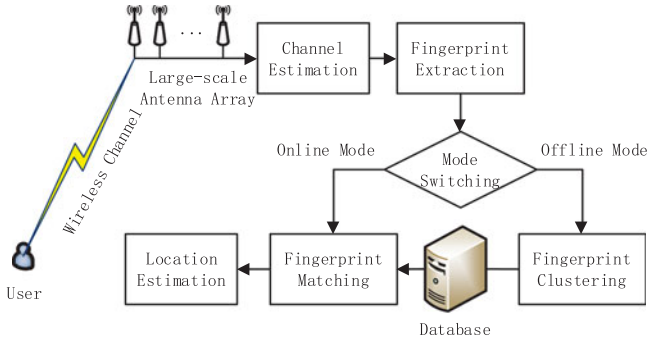

Fig. 1. General system model of the fingerprint wireless localization method.

For fingerprint extraction, there are two major types of parameters used in previous works. The first one is RSS information from access points (APs), which is usually used in indoor wireless sensor networks (WSN) [12], [15], [18], [24] and WiFi network [17]. Since the RSS is coarse information, existing RSS fingerprint methods usually depend on multiple BSs cooperation to assure high localization accuracy [14], [16], [17], which can only be operated in indoor scenario with rich AP distribution. Further more, the RSS values may vary from time to time due to the fast fading fluctuation and multipath effects. The second type of parameters used as fingerprints is multipath characteristics, including channel state information (CSI) [19], [20], [23], AOA [13], power delay profile (PDP) [11] and their combination [21], [22]. Different from the RSS fingerprint, the multipath fingerprint extracts more details from each propagation link and exploits the multipath characteristics. As a consequence, fewer APs with multiple antennas are enough to assure the accuracy.

In this paper, we propose a fingerprint based single-site localization method for massive MIMO-OFDM systems, exploiting both the AOA and PDP parameters as our fingerprint. A general system model of our proposed fingerprint wireless localization method is demonstrated in Fig. 1. Without requirement for extra signal transmission, we extract the angle delay channel power matrix (ADCPM) as the fingerprint from channel estimation results. The rest of the system consists of two modes: the offline mode and the online mode. During the offline mode, a low-cost autonomous mobile terminal traverses the target area to acquire a grid of reference points. Then the fingerprints and the corresponding coordinates are clustered and saved into the database. During the online mode, the fingerprints of the mobile terminals who have localization demand are matched to the clustered fingerprints in the database. Then we can carry out location estimation based on the matching results.

Different from other fingerprint wireless localization methods in WSN and WiFi systems, fingerprint extraction and matching in massive MIMO-OFDM systems require even higher computational complexity due to higher multipath resolution in the angle and delay domains. Therefore, in this paper we concentrate on computational complexity reduction problems from two aspects. On the one hand, we develop an efficient fingerprint extraction method and the corresponding similarity criterion to reduce the computational complexity for each calculation. On the other hand, we exploit a clustering algorithm and a new location estimation method to improve location estimation with low computational complexity and latency. We now summarize our major contributions in four aspects.

1) We develop an ADCPM fingerprint extraction method and a corresponding fingerprint compression method. The ADCPM fingerprint has two major advantages. First, the ADCPM can be extracted easily from the channel estimation results through fast Fourier transform (FFT). Second, the ADCPM has rich multipath information with clear physical interpretation, as the channel power associated with the specific AOA and TOA. Thus we can exploit the sparse characteristics for fingerprint compression and clustering.
2) We propose a new fingerprint similarity criterion: joint angle delay similarity coefficient (JADSC), used for the distance calculation between two fingerprints. Statistically, the JADSC fingerprint criterion is a decreasing function of the physical distance so that we can backtrack from the distance between two fingerprints to the geographical distance between the two corresponding locations and carry out location estimation.
3) We develop a two-stage fingerprint clustering algorithm for database preprocessing. The algorithm exploits the spatial characteristics of fingerprints to significantly reduce the fingerprints matching operations. Through the database preprocessing, we can avoid searching through the whole database to find the most matched fingerprint and significantly reduce computational complexity and latency.
4) We exploit the weighted K-nearest neighbor (WKNN) method for accurate location estimation, which can improve the location eatimation accuracy with limited reference points.

The rest of the paper is organized as follows. In Section II, the channel model as well as the ADCPM fingerprint extraction method are presented. Then we propose the JADSC fingerprint similarity criterion in Section III. In Section IV, we develop a two-stage fingerprint clustering method for database preprocessing and a WKNN method for accurate location estimation. In Section IV, numerical results are provided to demonstrate the performance of the proposed localization method. Finally, in Section V, we conclude the paper.

II. Fingerprint Extraction

In this section, we present the channel model and the fingerprint extraction method in massive MIMO-OFDM systems. The BS is equipped with $N_t (\gg 1)$ antennas in the form of uniform linear array (ULA), and the CSI is assumed to be known at the BS through uplink channel estimation.

A. Channel Model

For simplicity and without loss of generality, we assume that the users are randomly distributed in the coverage area. The wireless channel from an arbitrary user k to the BS in Fig. 1 is further demonstrated in Fig. 2.

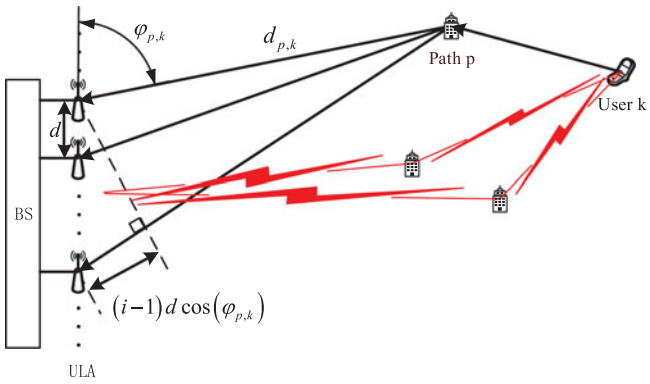

Fig. 2. Wireless channel from an arbitrary user k to the BS.

We assume the wireless signal propagates along multipath from $P(\gg 1)$ different scatterers to the BS, then the $N_t \times 1$ channel impulse response (CIR) vector associated with the pth path of the kth user is given by

$$\mathbf{q}_{p,k} = a_{p,k}\mathbf{e}\left(\varphi_{p,k}\right) e^{-j2\pi\frac{d_{p,k}}{\lambda_c}}, \tag{1}$$

where $a_{p,k} \sim \mathcal{CN}\left(0, \sigma_{p,k}\right)$ represents the complex gain associated with the pth path. $\varphi_{p,k} \in (0, \pi)$ and $d_{p,k}$ representing the AOA and the physical distance between the transmit antenna and the first receive antenna associated with the pth path, respectively, and λ_c is the carrier wavelength. As shown in Fig. 2, the array response vector corresponding to the AOA can be expressed as

$$\mathbf{e}\left(\varphi\right) = \left[1, e^{-j2\pi\frac{d_s\cos(\varphi)}{\lambda_c}}, \ldots, e^{-j2\pi\frac{(N_t-1)d_s\cos(\varphi)}{\lambda_c}}\right]^T, \tag{2}$$

where d_s is the antenna spacing. In the subsequent discussion, we will further assume that the scatterers are uniformly and independently distributed in the sector, and thus large scale parameters, such as the AOAs, $\varphi_{p,k}$, and the phases, $\frac{2\pi d_{p,k}}{\lambda_c}$, are independent from each other.

Define a phase-shifted discrete Fourier transform (DFT) matrix $\mathbf{V} \in \mathbb{C}^{N_t \times N_t}$ as $[\mathbf{V}]_{i,j} \triangleq \frac{1}{\sqrt{N_t}} e^{-j2\pi\frac{i(j-N_t/2)}{N_t}}$ and the angle domain CIR vector associated with the pth path of the kth user as $\tilde{\mathbf{q}}_{p,k} = \mathbf{V}^H\mathbf{q}_{p,k}$ [25]. The angle domain CIR, $\tilde{\mathbf{q}}_{p,k}$, can be interpreted as a mapping from the antenna domain to the angle domain, with each element indicating the channel gain of the corresponding AOA.

Property 1: When $N_t \to \infty$, the channel power of each path is concentrated on the $\left\lfloor \frac{N_t d_s\cos(\varphi_{p,k})}{\lambda_c} + \frac{N_t}{2} \right\rceil$th angle direction ($\lfloor x \rceil$ denotes the integer closest to x), with the average channel power

$$\mathbb{E}\left\{\left[\tilde{\mathbf{q}}_{p,k}\right]_i^2\right\} \to \begin{cases} N_t\sigma_{p,k}, & i = \frac{N_t d_s\cos(\varphi_{p,k})}{\lambda_c} + \frac{N_t}{2} \\ 0, & i \neq \frac{N_t d_s\cos(\varphi_{p,k})}{\lambda_c} + \frac{N_t}{2} \end{cases}. \tag{3}$$

Proof: The ith element of $\tilde{\mathbf{q}}_{p,k}$ can be calculated as

$$\begin{aligned}\left[\tilde{\mathbf{q}}_{p,k}\right]_i &= \frac{a_{p,k}}{\sqrt{N_t}} e^{-j2\pi\frac{d_{p,k}}{\lambda_c}} \sum_{m=0}^{N_t-1} e^{j2\pi\frac{m(i-N_t/2)}{N_t}} e^{-j2\pi\frac{m d_s\cos\left(\varphi_{p,k}\right)}{\lambda_c}} \\ &= \frac{a_{p,k}}{\sqrt{N_t}} e^{-j2\pi\frac{d_{p,k}}{\lambda_c}} e^{-j\pi(N_t-1)\left(\frac{d_s\cos\left(\varphi_{p,k}\right)}{\lambda_c} - \frac{i}{N_t} + \frac{1}{2}\right)} \\ &\quad \cdot \frac{\sin\left(\frac{N_t}{2}\left(\frac{d_s\cos\left(\varphi_{p,k}\right)}{\lambda_c} - \frac{i}{N_t} + \frac{1}{2}\right)\right)}{\sin\left(\frac{1}{2}\left(\frac{d_s\cos\left(\varphi_{p,k}\right)}{\lambda_c} - \frac{i}{N_t} + \frac{1}{2}\right)\right)}. \end{aligned} \tag{4}$$

When $\frac{N_t d\cos\left(\varphi_{p,k}\right)}{\lambda_c} + \frac{N_t}{2}$ equals an integer i_{center}, $\tilde{\mathbf{q}}_{p,k}$ has only one non-zero elements at the i_{center}th element since $\lim_{x\to 0}\frac{\sin(Ax)}{\sin(x)} = A$. As a reslut,

$$\left[\tilde{\mathbf{q}}_{p,k}\right]_{i_{center}} = \sqrt{N_t}a_{p,k}e^{-j2\pi\frac{d_{p,k}}{\lambda_c}}. \tag{5}$$

In this specific case, the channel power is concentrated on the i_{center}th DFT point. When $\frac{N_t d\cos\left(\varphi_{p,k}\right)}{\lambda_c} + \frac{N_t}{2}$ is not an integer, $\tilde{\mathbf{q}}_{p,k}$ can be regarded as the discrete samples of phase-shifted DFT of $\mathbf{q}_{p,k}$ corresponding to the AOA $\varphi_{p,k}$, whose leakage from the $\left\lfloor \frac{N_t d_s\cos\left(\varphi_{p,k}\right)}{\lambda_c} + \frac{N_t}{2} \right\rceil$th DFT point is proportional to the deviation $\left(\frac{N_t d\cos\left(\varphi_{p,k}\right)}{\lambda_c} + \frac{N_t}{2} - \left\lfloor \frac{N_t d_s\cos\left(\varphi_{p,k}\right)}{\lambda_c} + \frac{N_t}{2} \right\rceil\right)$ and is inversely proportional to the number of discrete samples N_t. Thus, when N_t tends to large, $\tilde{\mathbf{q}}_{p,k}$ can be approximated by a sparse vector with a few non-zero elements around the i_{center}th element. Specifically, when $N_t \to \infty$, $i_{center} \to \frac{N_t d\cos\left(\varphi_{p,k}\right)}{\lambda_c} + \frac{N_t}{2}$. Therefore,

$$\lim_{N_t\to\infty}\left[\tilde{\mathbf{q}}_{p,k}\right]_i = \begin{cases} \sqrt{N_t}a_{p,k}e^{-j2\pi\frac{d_{p,k}}{\lambda_c}}, & \\ \qquad i = \frac{N_t d_s\cos\left(\varphi_{p,k}\right)}{\lambda_c} + \frac{N_t}{2}, \\ 0, & \\ \qquad i \neq \frac{N_t d_s\cos\left(\varphi_{p,k}\right)}{\lambda_c} + \frac{N_t}{2}. \end{cases} \tag{6}$$

From the assumption that $a_{p,k} \sim \mathcal{CN}\left(0, \sigma_{p,k}\right)$, the channel power can be calculated as

$$\mathbb{E}\left\{\left[\tilde{\mathbf{q}}_{p,k}\right]_i^2\right\} \to \begin{cases} N_t\sigma_{p,k}, & i = \frac{N_t d_s\cos\left(\varphi_{p,k}\right)}{\lambda_c} + \frac{N_t}{2}, \\ 0, & i \neq \frac{N_t d_s\cos\left(\varphi_{p,k}\right)}{\lambda_c} + \frac{N_t}{2}. \end{cases} \tag{7}$$

□

Property 1 establishes a mapping from the antenna domain CIR to the angle domain CIR via the DFT, which enlightens us to extract the AOA characteristics from CSI known to the BS.

By employing OFDM modulation, the frequency-selective fading channel due to multipath propagation can be transformed to frequency-flat channel and the TOA of each path can be separated via time domain sampling. The relationship between the channel frequency response (CFR) and the CIR is given as follows.

Property 2: For OFDM systems, the CFR of the lth subcarrier can be denoted as the summation of the CIRs corresponding to each path as follows,

$$\mathbf{h}_{k,l} = \sum_{p=1}^{P} a_{p,k}\mathbf{e}\left(\varphi_{p,k}\right) e^{-j2\pi \frac{l n_{p,k}}{N_c}}, \tag{8}$$

where $n_{p,k} = \left\lfloor \frac{\tau_{p,k}}{T_s} \right\rfloor \bmod N_c$ denotes the temporally resolvable propagation delay associated with the pth path, $\tau_{p,k} = \frac{d_{p,k}}{v}$ is the TOA of each path, v is the speed of light, T_s and N_c are the sample interval and the number of subcarriers in the OFDM system, respectively.

Proof: Considering the TOA of each path, the CIR of the kth user can be denoted in terms of the underlying summation of the CIRs as follows

$$\mathbf{q}_k\left(\tau\right) = \sum_{p=1}^{P} \mathbf{q}_{p,k} \cdot \delta\left(\tau - \tau_{p,k}\right). \tag{9}$$

The outputs of the antenna array are sampled with the sample interval T_s such that $T_c = N_c T_s$ represents the OFDM symbol interval. The duration of the cyclic prefix is given by $T_g = N_g T_s$ where we assume T_g is larger than the maximum delay spread that $\tau_{p,k} \in [0, T_g)$. Then the bandwidth of each subcarrier is $f = \frac{1}{N_c T_s}$ and $f_l = lf$ for the lth subcarrier. The CFR is the Fourier transform of CIR, given by

$$\begin{aligned}\mathbf{h}_{k,l} &= \sum_{p=1}^{P} \sum_{n=0}^{N_g-1} a_{p,k}\mathbf{e}\left(\varphi_{p,k}\right) e^{-j2\pi f_l \tau_{p,k}} \cdot \delta\left(nT_s - \tau_{p,k}\right) \\ &= \sum_{p=1}^{P} a_{p,k}\mathbf{e}\left(\varphi_{p,k}\right) e^{-j2\pi \frac{l n_{p,k}}{N_c}}. \end{aligned} \tag{10}$$

□

From Property 2, the CFR is the summation of the time domain CIRs with different delays from the physical sense. Vice versa, we can extract the uncorrelated time domain CIRs from known CFR by inverse fast Fourier transform (IFFT), which has enlightening significance during fingerprint extraction.

Then the overall CFR matrix is given by

$$\mathbf{H}_k = \left[\mathbf{h}_{k,0}, \mathbf{h}_{k,1}, \ldots, \mathbf{h}_{k,N_c-1}\right]. \tag{11}$$

B. ADCPM Fingerprint Extraction

For fingerprint wireless localization, we need to extract the wide-sense stationary characteristics from the instantaneous CSI. From the aforementioned channel model, it is clear that the channel power corresponding to the propagation path fulfills our requirements, which includes the power, the AOA, and the TOA of each path. Motivated by Properties 1 and 2, we define the angle delay domain channel response matrix (ADCRM) as follows

$$\mathbf{G}_k = \mathbf{V}^H \mathbf{H}_k \mathbf{F}^*_{N_c \times N_g}, \tag{12}$$

where $\mathbf{F}_{N_c \times N_g} \in \mathbb{C}^{N_c \times N_g}$ denotes the matrix composed of the first N_g columns of N_c-dimensional unitary DFT matrix as $\left[\mathbf{F}_{N_c \times N_g}\right]_{i,j} \triangleq \frac{1}{\sqrt{N_c}} e^{-j2\pi \frac{ij}{N_c}}$. The left multiplication operator, $\mathbf{V}^H$, and the right multiplication operator, $\mathbf{F}^*_{N_c \times N_g}$, map the space frequency domain CFR to the angle domain and the delay domain separately. Thus, the (i, j)th element of the ADCRM represents the complex gain associated with the ith AOA and the jth TOA and satisfies the following property.

Theorem 1: When $N_t \to \infty$, the elements of the ADCRM are independent of each other. The statistical channel power associated with the ith AOA and the jth TOA is given as

$$\begin{aligned}\mathbb{E}\left\{\left|\left[\mathbf{G}_k\right]_{i,j}\right|^2\right\} = N_t \sum_{p=1}^{P} \sigma_{p,k} \cdot \delta\left(i - \frac{N_t d_s \cos\left(\varphi_{p,k}\right)}{\lambda_c} - \frac{N_t}{2}\right) \\ \cdot \delta\left(j - n_{p,k}\right). \end{aligned} \tag{13}$$

Proof: From Properties 1 and 2, the angle delay domain channel response can be calculated as

$$\begin{aligned}\left[\mathbf{G}_k\right]_{i,j} = \sum_{p=1}^{P} \frac{a_{p,k}}{\sqrt{N_t}} e^{-j\pi(N_t-1)\left(\frac{d_s \cos\left(\varphi_{p,k}\right)}{\lambda_c} - \frac{i}{N_t} + \frac{1}{2}\right)} \\ \cdot \frac{\sin\left(\frac{N_t}{2}\left(\frac{d_s \cos\left(\varphi_{p,k}\right)}{\lambda_c} - \frac{i}{N_t} + \frac{1}{2}\right)\right)}{\sin\left(\frac{1}{2}\left(\frac{d_s \cos\left(\varphi_{p,k}\right)}{\lambda_c} - \frac{i}{N_t} + \frac{1}{2}\right)\right)} \cdot \delta\left(n_{p,k} - j\right). \end{aligned} \tag{14}$$

From Property 1, when $N_t \to \infty$, for each path we can find an integer $i_{center} = \frac{N_t d \cos\left(\varphi_{p,k}\right)}{\lambda_c} + \frac{N_t}{2}$, such that all the channel power is concentrated at the i_{center}th element, given by (6). In this case, $\left[\mathbf{G}_k\right]_{i,j}$ can be calculated as the summation of the channel powers concentrated on the i_{center}th DFT point, given by

$$\lim_{N_t \to \infty} \left[\mathbf{G}_k\right]_{i,j} = \begin{cases} \sqrt{N_t} \sum\limits_{p=1}^{P} a_{p,k} \cdot \delta\left(n_{p,k} - j\right), \\ \qquad i = \frac{N_t d_s \cos\left(\varphi_{p,k}\right)}{\lambda_c} + \frac{N_t}{2}, \\ 0, \\ \qquad i \neq \frac{N_t d_s \cos\left(\varphi_{p,k}\right)}{\lambda_c} + \frac{N_t}{2}. \end{cases} \tag{15}$$

From the assumption that $a_{p,k} \sim \mathcal{CN}\left(0, \sigma_{p,k}\right)$, when $N_t \to \infty$, we have

$$\mathbb{E}\left\{\left[\mathbf{G}_k\right]_{i,j}\left[\mathbf{G}_k\right]_{i',j'}\right\} = \begin{cases} N_t \sum\limits_{p=1}^{P} \sigma_{p,k}, \\ \qquad i = i' = \frac{N_t d_s \cos\left(\varphi_{p,k}\right)}{\lambda_c} + \frac{N_t}{2} \\ \qquad \text{and } j = j' = n_{p,k} \quad , \\ 0, \\ \qquad \text{else.} \end{cases} \tag{16}$$

and

$$\begin{aligned}\mathbb{E}\left\{\left|\left[\mathbf{G}_k\right]_{i,j}\right|^2\right\} = N_t \sum_{p=1}^{P} \sigma_{p,k} \cdot \delta\left(i - \frac{N_t d_s \cos\left(\varphi_{p,k}\right)}{\lambda_c} - \frac{N_t}{2}\right) \\ \cdot \delta\left(j - n_{p,k}\right). \end{aligned} \tag{17}$$

□

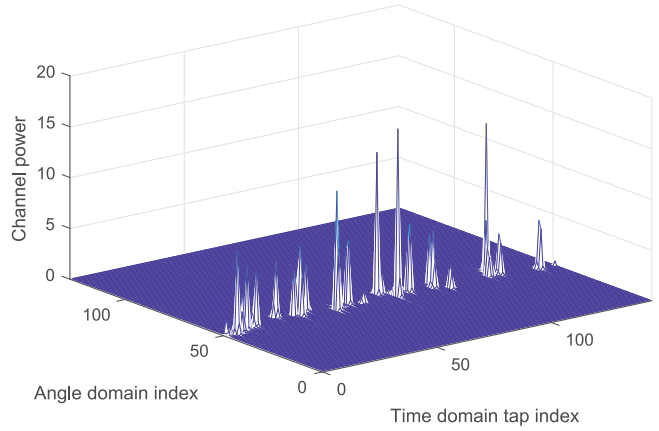

Fig. 3. Example of ADCPM with $N_t = 128$ and $N_g = 144$.

Now we define the angle delay channel power matrix (ADCPM) as

$$\mathbf{\Omega}_k \triangleq \mathbb{E}\left\{\mathbf{G}_k \odot \mathbf{G}_k^*\right\}, \tag{18}$$

where $\odot$ denotes the Hadamard product so that $[\mathbf{\Omega}_k]_{i,j} = \mathbb{E}\left\{\left|[\mathbf{G}_k]_{i,j}\right|^2\right\}$. From Theorem 1, the ADCPM makes a full-scale description of the channel power, the AOA, and the TOA of each path corresponding to the scattering environment of user k, as shown in Fig. 3. The ADCPM can be easily extracted from the CFR known to the BS via (12) and (18), and thus in the rest of the paper, we use the ADCPM together with the corresponding location information as our fingerprint for localization.

C. Fingerprint Compression

Many recent study and experiment results in massive MIMO systems have required BS to be elevated at a very high altitude with few scatterers surrounding the BS [6], [26], [27], and thus the scattering environment of each link from the user terminal to the BS is mainly determined by the nearest scatterers limited in a narrow region. Due to the limited distribution of scatterers relative to the large dimension of wireless channels, the wireless channels between the user terminals and the BS exhibit sparsity in both the angle domain and the delay domain according to Theorem 1. As a consequence, the ADCPM can be actually viewed as a sparse channel representation and we can significantly reduce the fingerprint storage overhead by employing matrix compression method, such as coordinate format (COO), compressed sensing (CS), and so on.

In this paper, considering the complexity of data compression and recovery, we will use COO method to compress the fingerprints in the database. In COO, we present a matrix with three rows: a value row, a row coordinate row, and a column coordinate row. For each fingerprint, we capture the largest $N\,(\ll N_t \times N_g)$ elements in the ADCPM and save their values and coordinates in the following structure,

$$\mathbf{F}_{compressed} = \begin{bmatrix} \text{value}_1 & \cdots & \text{value}_N \\ \text{x}_1 & \cdots & \text{x}_N \\ \text{y}_1 & \cdots & \text{y}_N \end{bmatrix}. \tag{19}$$

The compression ratio $R = \frac{N_t \times N_g}{3N}$ may vary for different scattering environments due to the sparsity of the ADCPMs. When a fingerprint is required from the database, we can easily recover the ADCPM through zero-padding with the compressed fingerprint.

III. Fingerprint Similarity Criterion

By extracting the ADCPM from the CFR known to the BS, we transform the localization problem into a pattern recognition problem, including the distance calculation between two fingerprints and the mapping from fingerprint distance to physical distance. Specifically for the distance calculation between two fingerprints, we require that the fingerprint similarity criterion be a decreasing function of the physical distance. In this section, we propose a new JADSC fingerprint similarity criterion and provide a theoretical justification.

We define the JADSC between location i and location j as:

$$J\left(\mathbf{\Omega}_\mathbf{i}, \mathbf{\Omega}_\mathbf{j}\right) \triangleq \max_{n\in(-L+1,L-1)} \left(\frac{1}{N_t^2}\sum_{t=1}^{N_g}[\mathbf{\Omega}_\mathbf{i}]_t^T[\mathbf{\Omega}_\mathbf{j}]_{t-n}\right), \tag{20}$$

where $[\mathbf{\Omega}]_t$ denotes the tth column of matrix $\mathbf{\Omega}$, n is the delay compensation between two fingerprints, and L is the maximum delay compensation. We employ the delay compensation and maximization operation to capture the maximum correlation between two fingerprints.

In massive MIMO-OFDM cellular systems, the BSs are always elevated at a very high altitude with few scatterers surrounding the BS, and thus the scattering environment of arbitrary location i is mainly determined by the P_i nearest local scatterers around location i. By taking (17) and (18) into (20), when N_t tends to large, we have

$$J\left(\mathbf{\Omega}_i, \mathbf{\Omega}_j\right) = \sum_{p_1=1}^{P_i}\sum_{p_2=1}^{P_j}\sigma_{p_1,i}\cdot\sigma_{p_2,j}\cdot\delta\left(\varphi_{p_1,i}-\varphi_{p_2,j}\right) \cdot\delta\left(n_{p_1,i}-n_{p_2,j}\right), \tag{21}$$

which indicates that the JADSC depends on the overlapping scatterers the two locations have.

Assume that the area of the target coverage is S, with M scatterers uniformly distributed in the targeted coverage. For each location, the scattering environment is determined by the P nearest scatterers and the channel power corresponding to each scatterer is identical, denoted as σ. Then the JADSC between location i and location j has the following property.

Theorem 2: For location i and location j with the physical distance d, the JADSC is a decreasing function of d, given by

$$J_d = \begin{cases} \frac{2P\sigma^2}{\pi}\arccos\left(\frac{d}{2}\sqrt{\frac{\pi M}{PS}}\right) - \frac{Md\sigma^2}{S}\sqrt{\frac{PS}{\pi M}-\frac{1}{4}d^2}, \\ \qquad 0 \le d < 2\sqrt{\frac{PS}{\pi M}}, \\ 0, \\ \qquad d \ge 2\sqrt{\frac{PS}{\pi M}}. \end{cases} \tag{22}$$

Proof: A simple system model of two locations with physical distance d is given in Fig. 4. From (21), the JADSC depends

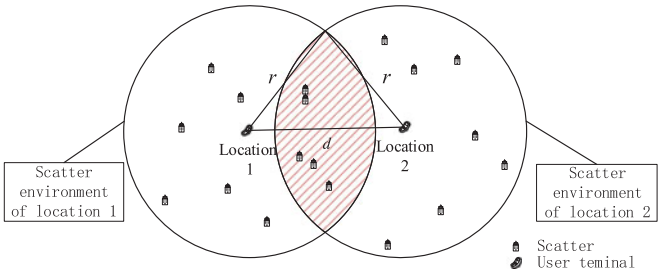

Fig. 4. Simple system model of two locations with physical distance d.

on the overlapping scatterers the two locations have, which is given by ■

$$J_d = \sigma^2 M \frac{S_{shadow}}{S}, \tag{23}$$

where S_{shadow} is the overlapping area of the scattering environments corresponding to each location. For each location, the radius of the scattering environment is given by

$$r = \sqrt{\frac{PS}{\pi M}}. \tag{24}$$

If $d \geq 2\sqrt{\frac{PS}{\pi M}}$, the scattering environments have no overlapping area, and thus $J_d = 0$. If $0 \leq d < 2\sqrt{\frac{PS}{\pi M}}$, the overlapping area of the scattering environments is calculated as

$$S_{shadow} = 2r^2 \arccos\left(\tfrac{d}{2r}\right) - d\sqrt{r^2 - \tfrac{1}{4}d^2}. \tag{25}$$

Substituting (24) and (25) into (23), we have

$$J_d = \frac{2P\sigma^2}{\pi} \arccos\left(\frac{d}{2}\sqrt{\frac{\pi M}{PS}}\right) - \frac{Md\sigma^2}{S}\sqrt{\frac{PS}{\pi M} - \frac{1}{4}d^2}. \tag{26}$$

The derivative of J_d is calculated as

$$\begin{aligned}\frac{\partial J_d}{\partial d} &= -\frac{P\sigma^2}{\pi}\sqrt{\frac{\pi M}{PS}}\frac{1}{\sqrt{1-\frac{d^2\pi M}{4PS}}} - \frac{M\sigma^2}{S}\left(\frac{PS}{\pi M} - \frac{1}{4}d^2\right)^{\frac{1}{2}} \\ &\quad + \frac{Md^2\sigma^2}{4S}\left(\frac{PS}{\pi M} - \frac{1}{4}d^2\right)^{-\frac{1}{2}} \\ &= -\frac{M\sigma^2}{S}\left(\frac{4PS}{\pi M} - d^2\right)^{\frac{1}{2}} \\ &< 0, \end{aligned} \tag{27}$$

which indicates that J_d is a decreasing function of d.

□

Theorem 2 provides a theoretical justification for our JADSC fingerprint similarity criterion. An example of JADSC distribution is given in Fig. 5. The reference point is located at $(26, 26)$ and the altitude corresponding to each location indicates the JADSC between the location and the reference point. From Fig. 5 we can see that the JADSC is a decreasing function of the physical distance. As a consequence, we can backtrack from the distances between fingerprints to the physical distances between the mobile terminals and the reference points in the database and carry out the location estimation.

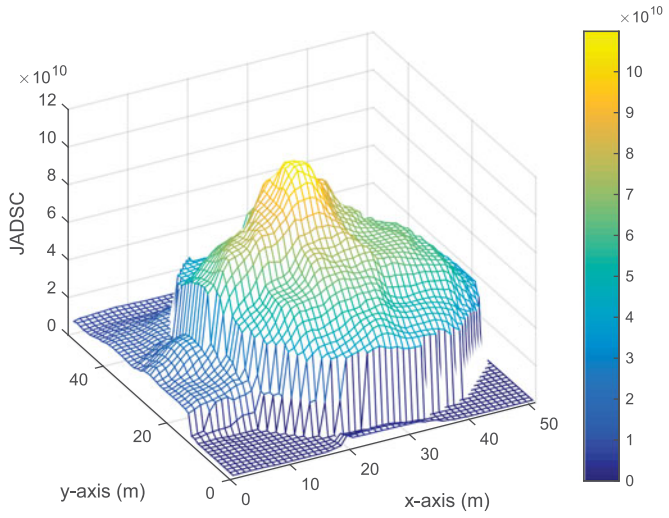

Fig. 5. Example of JADSC distribution.

IV. Fingerprint Clustering and Location Estimation

As any fingerprint based localization methods, the localization accuracy of our method depends on the density of reference points to some extent. During the offline mode, a low-cost autonomous mobile terminal traverses the target area to acquire hundreds of thousands of reference points to be stored in the database, resulting in enormous storage overhead. Whereas, given the fingerprint similarity criterion, we need to search through the whole database to find the most matched fingerprint for location estimation during the online mode, resulting in heavy computational burden and latency issues.

In Section II, we propose a COO method for fingerprint compression to significantly reduce the storage overhead. However, the heavy computational burden and latency problem for fingerprint matching is another stumbling block in the way of fingerprint localization. In order to solve the problem, in this section, we first propose a two-stage fingerprint clustering method for database preprocessing. To improve localization accuracy with limited reference points, we then propose a WKNN method for accurate location estimation. The proposed fingerprint clustering and location estimation algorithm is summarized in Table I and we will give a detailed explanation in the following.

A. Two-Stage Fingerprint Clustering

After collecting reference points and before the online phase, a two-stage fingerprint clustering can be performed as database preprocessing, which includes a spatial fingerprint classification and a K-means clustering. Since the database preprocessing is performed during the offline mode, the computation incurs no latency to the online mode location estimation operation.

The first stage clustering exploits the spatial characteristics of fingerprints. Since the scattering environment of each link from the user terminal to the BS is mainly determined by the nearest scatterers limited in a narrow region around the user terminal, as discussed in Section II, the incident angles of signal propagation paths for each user terminal exhibits a small angle spread seen from the BS. Note that the column vectors of ADCPM describe

TABLE I
FINGERPRINT CLUSTERING AND LOCATION ESTIMATION

Algorithm 1: Fingerprint Clustering and Location Estimation.

1: **Offline mode**
2: First stage clustering: For each fingerprint, calculate the center angle $\alpha_m \triangleq \arg\max_m \sum_{t=1}^{N_g} [\mathbf{\Omega}]_{m,t}$, and classify it into all the classes of the range $[\alpha_m - \alpha_0, \alpha_m + \alpha_0]$.
3: Second stage clustering: Initialization: For each class generated by the first stage clustering with N fingerp rints, randomly pick M ADCPMs as the initial mean. Set the iteration index $t = 0$, the iteration stopping toler ance ε, the initial sum JADSC $Sum_m^{(0)} = 0$ and the maximum number of iterations T_{max}.
4: **while** $t = 0$ or ($\left|Sum_m^{(t)} - Sum_m^{(t-1)}\right| > \varepsilon$ and $t < T_{max}$) **do**
5: Set $t = t + 1$.
6: Assign each fingerprint to the cluster whose mean has the largest JADSC with the fingerprint, $\mathbf{S}_m^{(t)} = \{\mathbf{\Omega}_n : J(\mathbf{\Omega}_n, \bar{\mathbf{\Omega}}_m) \geq J(\mathbf{\Omega}_n, \bar{\mathbf{\Omega}}_{m'}) \, \forall m', 1 \leq m' \leq M\}$.
7: Update the sum JADSC, $Sum_m^{(t)} = \sum_{m=1}^{M} \sum_{n \in \mathbf{S}_m} J(\mathbf{\Omega}_n, \bar{\mathbf{\Omega}}_m)$.
8: Update the new means of each cluster, $\bar{\mathbf{\Omega}}_m^{(t+1)} = \frac{1}{\left|\mathbf{S}_m^{(t)}\right|} \sum_{n \in \mathbf{S}_m^{(t)}} \mathbf{\Omega}_n$.
9: **end while**
10: **Online mode**
11: Calculate the center angle $\alpha_m \triangleq \arg\max_m \sum_{t=1}^{N_g} [\mathbf{\Omega}]_{m,t}$ and find the best-matched class.
12: Calculate the JADSCs between the fingerprint and the means of all clusters in the class and find out the nearest $N_{cluster}$ clusters.
13: Emerge the $N_{cluster}$ clusters to form a reference point pool and search through the point pool to find out the K nearest reference points.
14: Calculate and return the location estimation, $\hat{\mathbf{p}} = \sum_{i=1}^{K} w(\mathbf{\Omega}, \mathbf{\Omega}_i)\mathbf{p}_i$.

the channel power distribution in the angle domain, as shown in Fig. 3. Moreover, the channel power distribution remains nearly the same for different TOA. Thus, we define the center angle of ADCPM m as

$$\alpha_m \triangleq \arg\max_m \sum_{t=1}^{N_g} [\mathbf{\Omega}]_{m,t}, \tag{28}$$

where α_m indicates the index of the AOA on which the channel power mainly concentrates. Considering the angle spread of each user terminal, the actual location of user terminal m may lie in the angle range $[\alpha_m - \alpha_0, \alpha_m + \alpha_0]$ and α_0 is the maximum angle shift. Now we can perform the first stage spatial fingerprint classification based on the center angle of ADCPMs. Each fingerprint can be classified into several classes due to the consideration of angle spread. For example, the fingerprint m will be classified into all classes of range $[\alpha_m - \alpha_0, \alpha_m + \alpha_0]$.

For the second stage clustering, a K-means clustering method is employed since we can hardly find a concise label for classification. K-means clustering method is usually used to partition N observations into M clusters in which each observation belongs to the cluster with the nearest mean. However, for our fingerprint clustering problem, the distance calculation criterion will be replaced by the JADSC. For any class generated by the first stage clustering with N fingerprints, formally, the objective is to find

$$\arg\max_{\mathbf{S}} \sum_{m=1}^{M} \sum_{n \in \mathbf{S}_m} J(\mathbf{\Omega}_n, \bar{\mathbf{\Omega}}_m), \tag{29}$$

where $\mathbf{\Omega}_n$ is the ADCPM of user terminal n and $\bar{\mathbf{\Omega}}_m$ is the mean of the ADCPMs in cluster m.

The standard K-means clustering method is carried out as an iterative process including an assignment step and two update steps. During the second stage clustering, we firstly initialize the iterative process by randomly picking M ADCPMs from the class generated by the first stage clustering with N fingerprints as the initial mean. Then we set the iteration index $t = 0$, the iteration stopping tolerance ε, the initial sum JADSC $Sum_m^{(0)} = 0$ and the maximum number of iterations T_{max}. Repeat the following iterative process while $t = 0$, or $\left|Sum_m^{(t)} - Sum_m^{(t-1)}\right| > \varepsilon$ and the iteration index $t < T_{max}$.

1) *Assignment step:* Assign each fingerprint to the cluster whose mean has the largest JADSC with the fingerprint, given as

$$\mathbf{S}_m^{(t)} = \left\{ \begin{array}{c} \mathbf{\Omega}_n : J(\mathbf{\Omega}_n, \bar{\mathbf{\Omega}}_m) \geq J(\mathbf{\Omega}_n, \bar{\mathbf{\Omega}}_{m'}) \\ \forall m', 1 \leq m' \leq M \end{array} \right\}, \tag{30}$$

where $\mathbf{S}_m^{(t)}$ denotes the mth cluster after the tth iteration.

2) *Update step 1:* Calculate the sum JADSC

$$Sum_m^{(t)} = \sum_{m=1}^{M} \sum_{n \in \mathbf{S}_m} J(\mathbf{\Omega}_n, \bar{\mathbf{\Omega}}_m). \tag{31}$$

3) *Update step 2:* Calculate the new means of each cluster

$$\bar{\mathbf{\Omega}}_m^{(t+1)} = \frac{1}{\left|\mathbf{S}_m^{(t)}\right|} \sum_{n \in \mathbf{S}_m^{(t)}} \mathbf{\Omega}_n. \tag{32}$$

Now we give a brief analysis on the computational complexity for fingerprints matching operation. Since the two-stage fingerprint clustering process is carried out offline, the database preprocessing computational complexity is not our focus. The online computational complexity for each user's fingerprints matching operation is $\mathcal{O}\left((2L-1)N_t N_g \left(M + \frac{N_{Ref} N_{cluster}}{N_t M}\right)\right)$, where $(2L-1)N_t N_g$ is the computations for each JADSC calculation, M is the operations to find out the nearest $N_{cluster}$ clusters , $\frac{N_{Ref} N_{cluster}}{N_t M}$ is

the operations to find out the nearest reference points, and N_{Ref} is the total number of reference points.

In contrast, without the two-stage fingerprint matching algorithm, each user must search through the whole databese to find out the nearest reference points, with a computational complexity of $\mathcal{O}\left((2L-1)N_tN_gN_{Ref}\right)$. The complexity ratio is given by

$$R_c = \left(M + \frac{N_{\mathrm{Ref}}N_{cluster}}{N_tM}\right)\Big/ N_{\mathrm{Ref}} = \frac{M}{N_{\mathrm{Ref}}} + \frac{N_{cluster}}{N_tM}, \tag{33}$$

Since $M \ll N_{\mathrm{Ref}}$ and $N_{cluster} \ll N_tM$, we know that $R_c \ll 1$. The complexity ratio indicates that we can avoid searching through the whole database to find the most matched fingerprint and significantly reduce computational complexity and latency through the database preprocessing.

B. WKNN Location Estimation

The classical K-nearest neighbor (KNN) method has been widely used in fingerprint wireless localization and can provide excellent accuracy guarantee given enough reference points. The location estimation using the KNN method is given by

$$\hat{\mathbf{p}} = \frac{1}{K}\sum_{i=1}^{K}\mathbf{p}_i, \tag{34}$$

where $\mathbf{p}_i$ is the coordinate of the ith nearest reference point in the database. However, considering the fingerprint extraction and storage overhead, the number of reference points is usually limited in a fingerprint wireless localization system. As a result, the KNN method suffers from insufficient reference points. Motivated by this, we propose a weighted KNN method to use fewer reference points for location estimation with the consideration of the distance between the user terminal and different reference points. The location estimation using the WKNN method is given by

$$\hat{\mathbf{p}} = \sum_{i=1}^{K} w\left(\mathbf{\Omega}, \mathbf{\Omega}_i\right)\mathbf{p}_i, \tag{35}$$

where $w\left(\mathbf{\Omega}, \mathbf{\Omega}_i\right)$ is the weight factors meeting the following constraint conditions:

1) $\sum_{i=1}^{K} w\left(\mathbf{\Omega}, \mathbf{\Omega}_i\right) = 1$,
2) $w\left(\mathbf{\Omega}, \mathbf{\Omega}_i\right)$ is a decreasing function of physical distance d_i.

Here, we choose $w\left(\mathbf{\Omega}, \mathbf{\Omega}_i\right) = \frac{J(\mathbf{\Omega}, \mathbf{\Omega}_i)}{\sum_{i=1}^{K} J(\mathbf{\Omega}, \mathbf{\Omega}_i)}$ to meet the constraint conditions. As we can see, Condition 1 comes from the normalization operation and Condition 2 comes from Theorem 2 in that the JADSC function is a decreasing function of d.

During the online mode, for each fingerprint for localization, we first calculate the center angle of the ADCPM and find the best-matched class. Then we calculate the JADSCs between the fingerprint and the means of all clusters in the class and find out the nearest L clusters. After that we emerge the L clusters to form a reference point pool and search through the point pool to find out the K nearest reference points. Finally, we calculate location estimation by (35).

TABLE II
MAJOR WIRELESS PARAMETERS USED IN THE SIMULATION

Parameter	Value
Transmission bandwidth	5–80 MHz
Sub-carrier spacing	15 kHz
Sampling interval	$1/(2 \cdot bandwidth)$
Guard interval	4.7 μs
Number of antennas	8–256
Reference interval	1–5
Fingerprint compress ratio	100
K-means clustering stopping tolerence	0.002

V. SIMULATION RESULTS

In this section, we provide simulation results to evaluate the performance of the proposed fingerprint wireless localization method. A geometry-based 3D ray tracing signal propagation method is adopted to describe the multipath propagation so that the database and the user terminal fingerprints are generated in the same wireless propagation environment.

A. Simulation Environment

To simulate a typical urban wireless propagation scenario, we assume that each cell, with radius $R = 500$ m, is devided into three 120° sectors and the BS equipped with a ULA is located at the center of the cell. M scatterers are uniformly distributed in the sector and remain unchanged during the whole localization process. A 3D ray tracing signal propagation method is adopted to describe the multipath propagation so that the large scale parameters are determined by the corresponding scatterers. According to the recent study and experiment results in massive MIMO systems [6], [26], [27], the scattering environment of each link from the user terminal to the BS is mainly determined by the nearest scatterers limited in a narrow region. Without loss of generality, we take only the scatterers within a scatterer ring of $R_{scat} = 20$ m into consideration. The wireless parameters used in the simulation are set to those typical ones in the LTE-Advanced [28]–[30], as listed in Table II.

A single path from a user terminal to the BS through a scatterer consists of multi-points scattering, referred to as a subpaths cluster in 3GPP TR 36.814 [28]. For each cluster, the delay obeys exponential delay distribution with corresponding factors defined in [28, Table B.1.2.2.1–4] and the cluster power is calculated assuming a single slope exponential power delay profile. Each cluster has 40 scattering points uniformly distributed in a circle around the cluster center with radius $R_c = 3$ m. For each subpath, the delay is calculated by adding a small delay spread to the delay of the path and the AOA is calculated according to the scattering point location. Then the CFR of each user terminal is calculated by step-by-step accumulation from subpath to single path and from single path to overall CFR according to (1), (8) and (10).

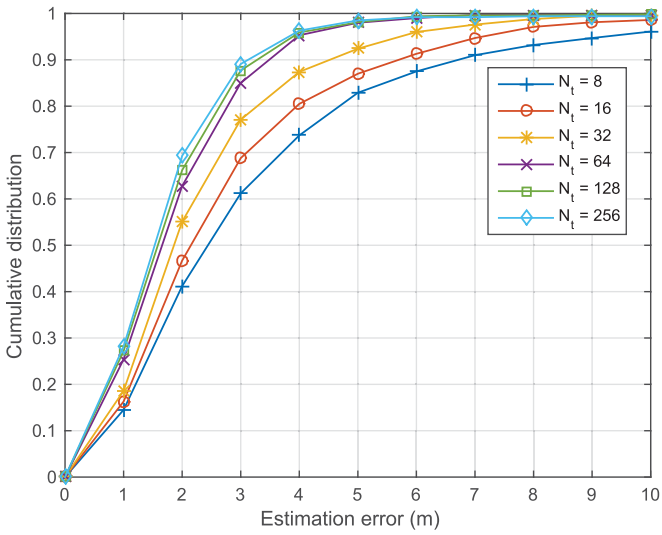

Fig. 6. CDF of the location errors with different number of BS antennas.

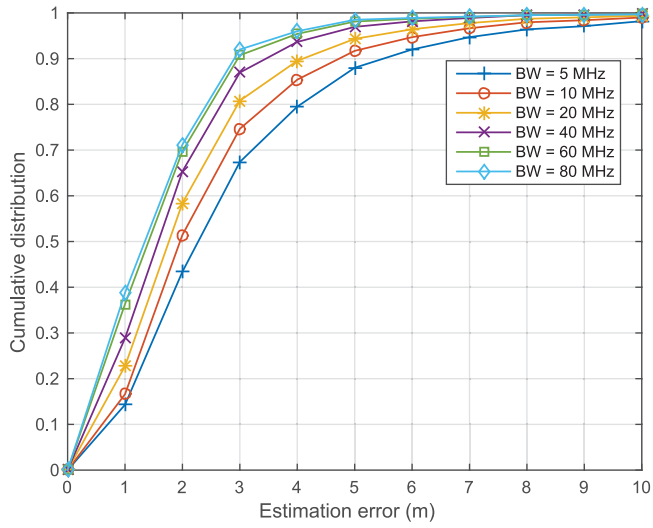

Fig. 7. CDF of the location errors with different transmission bandwidth.

The coverage area is uniformly gridded by the reference points with an interval s and the mobile terminals to be located are randomly distributed in the sector. During the offline mode, we extract the fingerprints of the grid of reference points and then save the fingerprints and the corresponding coordinates into the database. During the online mode, we extract the fingerprints of the mobile terminals and estimate the locations with our WKNN method. Then we compare the estimated locations with the true locations and compute the cumulative distribution function (CDF) of the location errors to evaluate the performance of the proposed fingerprint wireless localization system.

B. Simulation Results

With the above settings, we first evaluate the impact of the number of BS antennas on the localization accuracy when the number is increased from 8 to 256. The reference point interval is 2 m, the transmission bandwidth is 40 mHz, the compress ratio is 50, and the WKNN method with $K = 3$ neighbours is adopted. Fig. 6 shows that the accuracy of our proposed fingerprint localization method improves with the increase of BS antennas. Taking the 85% point of the CDF as a reference point for reliability, the figure indicates that a single BS with as few as 64 antennas can realize localization with 3 m accuracy. In the future massive MIMO-OFDM systems, the BS will be equipped with more than 100 antennas and therefore, our proposed method can offer 95% reliability for 4 m accuracy and 65% reliability for 2 m accuracy.

Next, we evaluate the impact of transmission bandwidth in Fig. 7. The transmission bandwidth is increased from 5 mHz to 60 mHz. The reference point interval is 2 m, the number of BS antennas is 64, the compress ratio is 50, and the WKNN method with $K = 3$ neighbours is adopted. From Fig. 7, the accuracy of our proposed fingerprint localization method improves with the increase of transmission bandwidth. For typical OFDM systems, the transmission bandwidth is usually set to be $20 - 100$ MHz and therefore, our proposed method can offer 90% reliability for 3 m accuracy with 60 mHz bandwidth and 80% reliability for 3 m accuracy with 20 mHz bandwidth.

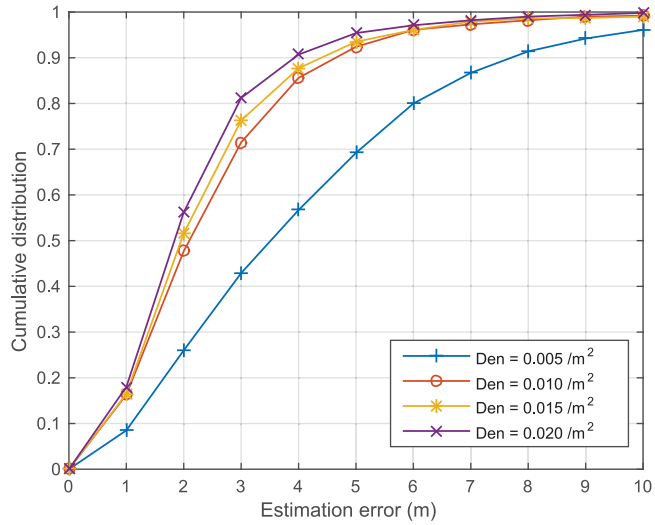

Fig. 8. CDF of the location errors with different scatterer density.

From the above results, we notice that the performance of our proposed fingerprint method exhibits bottleneck with the increase of number of BS antennas and transmission bandwidth. The high angle and delay domains resolution offered by massive MIMO systems has different gain due to different scatterer density. Thus we evaluate the effect of different scatterer density on the localization accuracy. The scatterer density is quantified by the number of scatterers per square meter. The scatterer density is increased from $0.005/\mathrm{m}^2$ to $0.02/\mathrm{m}^2$. The reference point interval is 2 m, the number of BS antennas is 64, the transmission bandwidth is 40 mHz, the compress ratio is 50, and the WKNN method with $K = 3$ neighbours is adopted. From Fig. 8, our proposed fingerprint localization method gains a performance improvement with the increase of scatterer density, which demonstrates that our ADCPM fingerprint can make full use of the rich multipath information for location estimation.

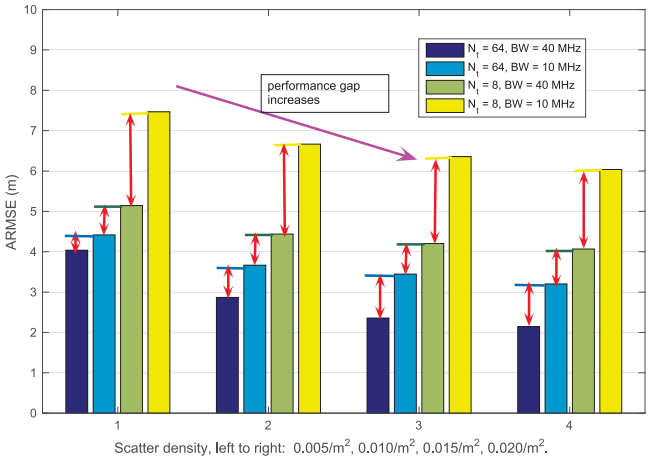

Fig. 9. ARMSE of differnet BS antennas and transmission bandwidth combination in different scatterering environment.

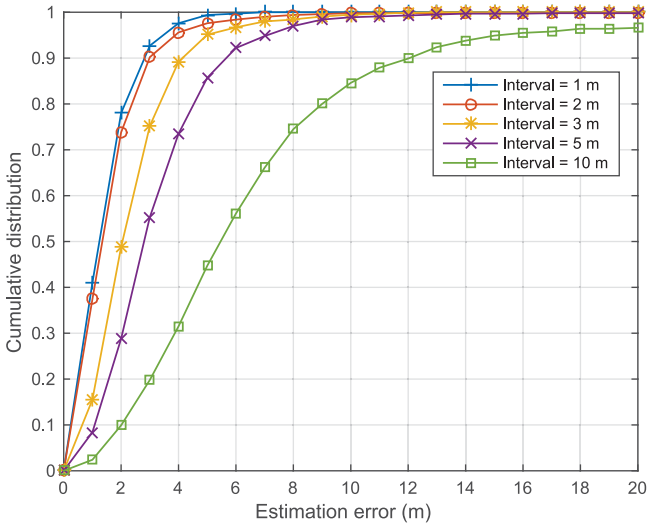

Fig. 10. CDF of the location errors with different reference point intervals.

We further compare different BS antennas and transmission bandwidth combinations in different scattering environments in Fig. 9. The standard of average root mean square error (ARMSE) is employed to measure the average localization accuracy. We choose four different BS antennas and transmission bandwidth combinations to form a control group performing our localization method in different scattering environments. The first bar of each comparison has high angle and delay domains resolution, the second one has high angle domain resolution but low delay domain resolution, the third one has low angle domain resolution but high delay domain resolution, and the last one has low angle and delay domains resolution. As we can see from Fig. 9, the ARMSEs of all four combinations decrease as the increase of the scatter density, which is consistent with the results in Fig. 8.

When we compare the performance gap between the same bars in different group, we can find that with higher angle and delay domains resolution, the performance of the first combination improves significantly with the increase of scatter density. On the other hand, the control groups with low angle and delay domains resolution can not make full use of the rich scattering environments. For example, the performance gap between the first bars in Group 1 and Group 4 is 2 m while the performance gap between the fourth bars in Group 1 and Group 4 is 1.4 m, which indicates that the benefits of rich scattering environments can be better used by the combination with more BS antennas and wider transmission bandwidth.

When we compare the performance gap between different bars within the same group, we can find that the performance gaps between different combinations increase with the scatter density. For example, the performance gap between the first two bars in Group 1 is 0.4 m while with a higher scatter density in group 4 the corresponding performance gap is 1 m, which indicates that the benefits of rich scattering environments can be better used by a wider transmission bandwidth offering a higher delay domain resolution.

In Fig. 10, we evaluate the impact of reference point interval. The reference point interval is increased from 1 m to 10 m. The transmission bandwidth is 80 mHz, the number of BS antennas is 128, the compress ratio is 50, and the WKNN method with $K = 3$ neighbours is adopted. From Fig. 10, a smaller reference point interval brings higher reliability for the same accuracy. For example, an interval of 3 m can offer a 90% reliability for 4 m accuracy while an interval of 1 m can offer as high as 98% reliability, with the cost of nine times reference points overhead. This makes sense since smaller reference point interval requires more fingerprints to be measured and saved during the offline mode as well as more matching overheads during the online mode. Thus we may choose a reasonable reference point interval depending on the accuracy requirement.

Finally, our fingerprint based localization method is compared to the conventional AOA based triangulation method [8] and the direct localization method [10]. Since both methods depend on multiple BSs cooperation, we reshape our simulation scenario to a 400 m $\times$ 400 m square between coordinates $[-200\,\text{m}, -200\,\text{m}]$, $[-200\,\text{m}, 200\,\text{m}]$, $[200\,\text{m}, 200\,\text{m}]$ and $[200\,\text{m}, -200\,\text{m}]$. Four BSs are located at coordinates $[-250\,\text{m}, 0\,\text{m}]$, $[250\,\text{m}, 0\,\text{m}]$, $[0\,\text{m}, -250\,\text{m}]$ and $[0\,\text{m}, 250\,\text{m}]$. Each BS is equipped with a 128-antenna ULA. The major wireless parameters are generated by the same channel coefficients as in Section V-A. The following methods are evaluated in our simulation.

1) TF-MUSIC [8]: Use joint diagonalization algorithm on a combined set of spatial temporal correlation matrices to estimate the direction of arrival (DOA). The DOA is determined by the strongest peak in the MUSIC spectrum and the location estimation is given by the intersection of DOAs from different BSs using triangulation.
2) DiSouL [10]: Use compress sensing framework to detect the LOS components from multipath. Coarse TOA estimation is exploited to narrow the feasible area. DiSouL is a direct localization approach that estimates the location directly from the data, instead of estimating intermediate parameters.
3) FPS: Use our fingerprint based method with single BS.

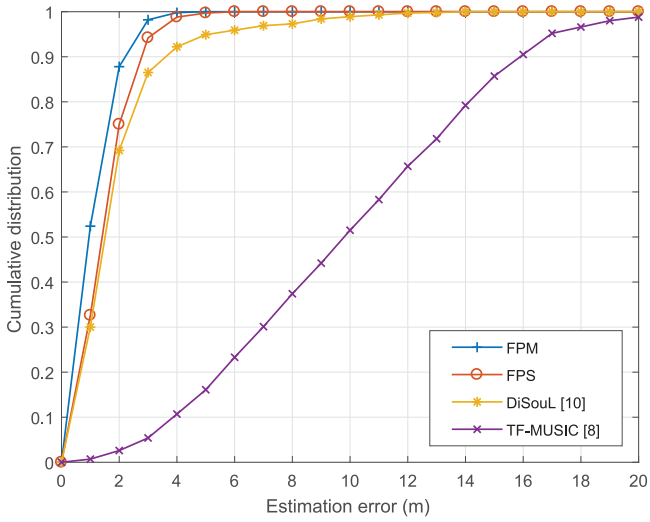

Fig. 11. CDF of the location errors with different localization methods.

4) FPM: Use our fingerprint based method with multiple BSs. Four BSs carried out our fingerprint based method independently and we choose the mean of the nearest three estimation results as the final estimated location.

From Fig. 11, the performance of our fingerprint based method with multiple BSs achieves the highest accuracy, with a 90% reliability for 2 m accuracy. The second is our fingerprint based method with single BS, offering a 75% reliability for 2 m accuracy and 95% reliability for 3 m accuracy. By exploiting multiple BSs cooperation, our fingerprint based method can further avoid accidental mismatching during online mode. The direct localization approach, DiSouL, achieves a 70% reliability for 2 m accuracy but remains a few large estimation errors caused by the absence of LOS path. The TF-MUSIC method performs far behind the other three methods, for the strongest peak in the MUSIC spectrum is not always the LOS path. Our fingerprint based method is the only approach that can offer reliable localization service with only single BS and have better versability when localization requirements emerge at non-overlapping areas.

VI. Conclusion

In this paper, we have investigated the fingerprint-based single-site localization method for massive MIMO-OFDM systems. To extract the wide-sense stationary characteristics from the instantaneous CSI, we have proposed an ADCPM fingerprint extraction method without extra signal transmission. Also, a new fingerprint similarity criterion JADSC with a theoretical justification has been proposed to evaluate the distance between two fingerprints. To reduce the storage overhead and the matching latency, a preprocessing method including fingerprint compression and two-stage fingerprint clustering has been developed. Last, a new WKNN location estimation method has been proposed to further improve the location estimation with limited reference points. Numerical results demonstrate the performance of the proposed localization method.

References

[1] A. H. Sayed, A. Tarighat, and N. Khajehnouri, "Network-based wireless location: challenges faced in developing techniques for accurate wireless location information," *IEEE Signal Process. Mag.*, vol. 22, no. 4, pp. 24–40, Jun. 2005.

[2] A. Roxin, J. Gaber, M. Wack, and A. Nait-Sidi-Moh, "Survey of wireless geolocation techniques," in *Proc. IEEE Globecom Workshops*, Nov. 2007, pp. 1–9.

[3] T. L. Marzetta, "Noncooperative cellular wireless with unlimited numbers of base station antennas," *IEEE Trans. Wireless Commun.*, vol. 9, no. 11, pp. 3590–3600, Nov. 2010.

[4] L. Lu, G. Y. Li, A. L. Swindlehurst, A. Ashikhmin, and R. Zhang, "An overview of massive MIMO: Benefits and challenges," *IEEE J. Sel. Areas Commun*, vol. 8, no. 5, pp. 742–758, Oct. 2014.

[5] H. Q. Ngo, E. G. Larsson, and T. L. Marzetta, "Energy and spectral efficiency of very large multiuser MIMO systems," *IEEE Trans. Commun.*, vol. 61, no. 4, pp. 1436–1449, Apr. 2013.

[6] A. Hu, T. Lv, H. Gao, Z. Zhang, and S. Yang, "An ESPRIT-based approach for 2-D localization of incoherently distributed sources in massive MIMO systems," *IEEE J. Sel. Topics Signal Process.*, vol. 8, no. 5, pp. 996–1011, Oct. 2014.

[7] T. Lv, F. Tan, H. Gao, and S. Yang, "A beamspace approach for 2-D localization of incoherently distributed sources in massive MIMO systems," *Signal Process.*, vol. 121, pp. 30–45, Apr. 2016.

[8] L. Hachad, O. Cherrak, H. Ghennioui, F. Mrabti, and M. Zouak, "DOA estimation based on time-frequency music application to massive MIMO systems," in *Proc. Int. Conf. Adv. Technol. Signal Image Process.*, May 2017, pp. 1–5.

[9] D. Liu, K. Liu, Y. Ma, and J. Yu, "Joint TOA and DOA localization in indoor environment using virtual stations," *IEEE Commun. Lett.*, vol. 18, no. 8, pp. 1423–1426, Aug. 2014.

[10] N. Garcia, H. Wymeersch, E. G. Larsson, A. M. Haimovich, and M. Coulon, "Direct localization for massive MIMO," *IEEE Trans. Signal Process.*, vol. 65, no. 10, pp. 2475–2487, May 2017.

[11] M. Triki, D. T. Slock, V. Rigal, and P. François, "Mobile terminal positioning via power delay profile fingerprinting: Reproducible validation simulations," in *Proc. IEEE Veh. Technol. Conf.*, Sep. 2006, pp. 1–5.

[12] M. Sugano, T. Kawazoe, Y. Ohta, and M. Murata, "Indoor localization system using RSSI measurement of wireless sensor network based on ZigBee standard," *Target*, vol. 538, 2006, Art. no. 050.

[13] M. Nezafat, M. Kaveh, and H. Tsuji, "Indoor localization using a spatial channel signature database," *IEEE Antennas Wireless Propag. Lett.*, vol. 5, no. 1, pp. 406–409, Dec. 2006.

[14] A. Kushki, K. N. Plataniotis, and A. N. Venetsanopoulos, "Kernel-based positioning in wireless local area networks," *IEEE Trans. Mobile Comput.*, vol. 6, no. 6, pp. 689–705, Jun. 2007.

[15] G. Mao, *Localization Algorithms and Strategies for Wireless Sensor Networks: Monitoring and Surveillance Techniques for Target Tracking: Monitoring and Surveillance Techniques for Target Tracking*. Hershey, PA, USA: IGI Global, 2009.

[16] R. W. Ouyang, A. K.-S. Wong, and C.-T. Lea, "Received signal strength-based wireless localization via semidefinite programming: Noncooperative and cooperative schemes," *IEEE Trans. Veh. Technol.*, vol. 59, no. 3, pp. 1307–1318, Jan. 2010.

[17] J. Biswas and M. Veloso, "Wifi localization and navigation for autonomous indoor mobile robots," in *Proc. IEEE Int. Conf. Robot. Autom.*, May 2010, pp. 4379–4384.

[18] L. Gogolak, S. Pletl, and D. Kukolj, "Indoor fingerprint localization in WSN environment based on neural network," in *Proc. IEEE 9th Int. Symp. Intell. Syst. Informat.*, Sep. 2011, pp. 293–296.

[19] Z. Yang, Z. Zhou, and Y. Liu, "From RSSI to CSI: Indoor localization via channel response," *ACM Comput. Surveys*, vol. 46, no. 2, Nov. 2013, Art. no. 25.

[20] K. Wu, J. Xiao, Y. Yi, D. Chen, X. Luo, and L. M. Ni, "CSI-based indoor localization," *IEEE Trans. Parallel Distrib. Syst.*, vol. 24, no. 7, pp. 1300–1309, Jul. 2013.

[21] E. Kupershtein, M. Wax, and I. Cohen, "Single-site emitter localization via multipath fingerprinting," *IEEE Trans. Signal Process.*, vol. 61, no. 1, pp. 10–21, Jan. 2013.

[22] A. Jaffe and M. Wax, "Single-site localization via maximum discrimination multipath fingerprinting," *IEEE Trans. Signal Process.*, vol. 62, no. 7, pp. 1718–1728, Apr. 2014.

[23] X. Wang, L. Gao, S. Mao, and S. Pandey, "CSI-based fingerprinting for indoor localization: A deep learning approach," *IEEE Trans. Veh. Technol.*, vol. 66, no. 1, pp. 763–776, Jan. 2017.

[24] Q. Jiang, Y. Ma, K. Liu, and Z. Dou, "A probabilistic radio map construction scheme for crowdsourcing-based fingerprinting localization," *IEEE Sensors J.*, vol. 16, no. 10, pp. 3764–3774, May 2016.
[25] Y. Zhou, M. Herdin, A. M. Sayeed, and E. Bonek, "Experimental study of MIMO channel statistics and capacity via the virtual channel representation," Univ. Wisconsin-Madison, Madison, WI, USA, Feb. 2007.
[26] A. Adhikary, J. Nam, J.-Y. Ahn, and G. Caire, "Joint spatial division and multiplexing - The large-scale array regim," *IEEE Trans. Inf. Theory*, vol. 59, no. 10, pp. 6441–6463, Oct. 2013.
[27] C. Sun, X. Gao, S. Jin, M. Matthaiou, Z. Ding, and C. Xiao, "Beam division multiple access transmission for massive MIMO communications," *IEEE Trans. Commun.*, vol. 63, no. 6, pp. 2170–2184, Jun. 2015.
[28] 3GPP, TR 36.814 Ver. 9.0.0, "Further Advancements for E-UTRA Physical Layer Aspects (Release 9)," Mar. 2010.
[29] S. Sesia, I. Toufik, and M. Baker, *LTE: The UMTS Long Term Evolution, From Theory to Practice*. New York, NY, USA: Wiley, 2009.
[30] N. Miyazaki, S. Nanba, and S. Konishi, "MIMO-OFDM throughput performances on MIMO antenna configurations using LTE-based testbed with 100 MHz bandwidth," in *Proc. IEEE Veh. Technol. Conf.*, Sep. 2010, pp. 1–5.

Xiaoyu Sun (S'13) received the B.E. degree in electrical engineering from Tsinghua University, Beijing, China, in 2012. He is currently working toward the Ph.D. degree with the National Mobile Communications Research Laboratory, Southeast University, Nanjing, China. From October 2015 to October 2017, he was a visiting student with the Department of Electrical and Computer Engineering, Georgia Institute of Technology, Atlanta, GA, USA. His research interests include massive MIMO communications and wireless localization.

Xiqi Gao (S'92–AM'96–M'02–SM'07–F'15) received the Ph.D. degree in electrical engineering from Southeast University, Nanjing, China, in 1997.

He joined the Department of Radio Engineering, Southeast University, in April 1992. Since May 2001, he has been a Professor of information systems and communications. From September 1999 to August 2000, he was a visiting scholar with Massachusetts Institute of Technology, Cambridge, MA, USA, and Boston University, Boston, MA, USA. From August 2007 to July 2008, he visited the Darmstadt University of Technology, Darmstadt, Germany, as a Humboldt scholar. His current research interests include broadband multicarrier communications, MIMO wireless communications, channel estimation and turbo equalization, and multirate signal processing for wireless communications.

Dr. Gao received the Science and Technology Awards of the State Education Ministry of China in 1998, 2006 and 2009, the National Technological Invention Award of China in 2011, and the 2011 IEEE Communications Society Stephen O. Rice Prize Paper Award in the Field of Communications Theory. From 2007 to 2012, he served as an Editor for the IEEE TRANSACTIONS ON WIRELESS COMMUNICATIONS. From 2009 to 2013, he served as an Editor for the IEEE TRANSACTIONS ON SIGNAL PROCESSING. From 2015 to 2017, he served as an Editor for the IEEE TRANSACTIONS ON COMMUNICATIONS.

Geoffrey Ye Li (S'93–M'95–SM'97–F'06) received the B.S.E. and M.S.E. degrees in 1983 and 1986, respectively, from the Nanjing Institute of Technology, Nanjing, China, and the Ph.D. degree in 1994 from Auburn University, Auburn, AL, USA.

He was a Teaching Assistant and then a Lecturer with Southeast University, Nanjing, China, from 1986 to 1991, a Research and Teaching Assistant with Auburn University from 1991 to 1994, and a Postdoctoral Research Associate with the University of Maryland at College Park, College Park, MD, USA, from 1994 to 1996. He was with AT&T Labs—Research at Red Bank, Middletown, NJ, USA, as a Senior and then a Principal Technical Staff Member from 1996 to 2000. Since 2000, he has been with the School of Electrical and Computer Engineering, Georgia Institute of Technology, Atlanta, GA, USA, as an Associate Professor and then a Full Professor. He is also holding a Cheung Kong Scholar title with the University of Electronic Science and Technology of China since 2006. His general research interests include statistical signal processing and machine learning for wireless communications. In these areas, he has published over 200 journal papers in addition to over 40 granted patents and many conference papers.

Dr. Li's publications have been cited over 30 000 times and he has been recognized as the Worlds Most Influential Scientific Mind, also known as a Highly-Cited Researcher, by Thomson Reuters almost every year. He was awarded IEEE Fellow for his contributions to signal processing for wireless communications in 2005. He won 2010 IEEE ComSoc Stephen O. Rice Prize Paper Award, 2013 IEEE VTS James Evans Avant Garde Award, 2014 IEEE VTS Jack Neubauer Memorial Award, 2017 IEEE ComSoc Award for Advances in Communication, and 2017 IEEE SPS Donald G. Fink Overview Paper Award. He also received 2015 Distinguished Faculty Achievement Award from the School of Electrical and Computer Engineering, Georgia Tech. He has been involved in editorial activities for more than 20 technical journals for the IEEE, including founding Editor-in-Chief of IEEE 5G Tech Focus. He has organized and chaired many international conferences, including Technical Program Vice-Chair of IEEE ICC03, Technical Program Co-Chair of IEEE SPAWC11, General Chair of IEEE GlobalSIP14, and Technical Program Co-Chair of IEEE VTC16 (Spring).

Wei Han received the B.S. and Ph.D. degrees, both in electrical engineering, from Xi'an Jiaotong University, Xi'an, China, in 2004 and 2013, respectively. He is currently with Huawei Technology Co., Ltd, Shenzhen, China. His research interests include MIMO transceiver design, iterative detection/decoding, theory and application of optimization techniques, and software/hardware codesign implementation for general signal processing systems.